Available online at www.sciencedirect.com
SCIENCE DIRECT®
International Journal of Thermal Sciences 43 (2004) 1057–1065
International Journal of Thermal Sciences
www.elsevier.com/locate/ijts

Two-dimensional numerical simulation of thermo-gravitational convection in a vertical porous column filled with a binary fluid mixture

C.G. Jiang [a,b], M.Z. Saghir [a,*], M. Kawaji [b], K. Ghorayeb [c]

[a] *Ryerson University, Department of Mechanical Engineering, Ontario, Canada*
[b] *University of Toronto, Department of Chemical Engineering and Applied Chemistry, Ontario, Canada*
[c] *Schlumberger, Abingdon Technology Center, Abingdon, UK*

Received 13 August 2003; received in revised form 25 February 2004; accepted 3 March 2004

Available online 17 June 2004

Abstract

Convection has a very important effect on the thermal diffusion process in hydrocarbon porous media. We investigate the convection effect in a vertical cavity having an aspect ratio of 10 and subject to a lateral heating condition based on two-dimensional numerical simulation. Using the irreversible thermodynamics theory of Shukla and Firoozabadi [Ind. Engrg. Chem. Res. 37 (1998)], the space dependent thermal, molecular and pressure diffusion coefficients are calculated at each point of the grid as functions of the temperature, pressure and other properties of the mixture. The thermal diffusion process is simulated in a vertical porous media combined with natural convection flow over a range of permeability from 0.001 to 10 000 md. Numerical results reveal that the lighter fluid component migrates to the hot side of the cavity, and as the permeability increases, the component separation in the thermal diffusion, or Soret effect, process increases first, reaches its peak, and then decreases. This phenomenon is illustrated and discussed both numerically and physically.

Keywords: Convection; Soret effect; Thermodynamics; Separation; Control volume method

1. Introduction

In a uniform mixed binary mixture, when a temperature gradient is applied there appears a composition gradient. This thermal diffusion effect is named the Soret effect, and the ratio of the thermal diffusion coefficient to the molecular diffusion coefficient is known as the Soret coefficient, see Soret [1]. Usually, in a binary mixture, the lighter component migrates to the hot side. Theoretical developments related to the calculation of the molecular, thermal and pressure diffusion coefficients have received much attention by different researchers [2–10] in this field. Among these, Shukla and Firoozabadi [2], Riley et al. [5] and Ghorayeb et al. [6–8] using the irreversible thermodynamics theory, were able to extend the work of De Groot [9]. Ghorayeb et al. developed an analytical relation between the thermal, molecular and pressure diffusion coefficients and the properties of the fluid mixture, such as the temperature, pressure and composition. The advantage of this approach is that the Soret coefficient is calculated at each point of the cavity grid and all diffusion coefficients are completely defined. Compared with other approaches, such as Rutherford and Roof [10], the theoretical prediction of this approach is much closer to experimental data, especially for non-ideal mixtures, such as hydrocarbon mixtures.

Because of the complicated combination of different diffusion factors, the majority of previous studies on the Soret effect have investigated mainly the gravitational effect on the composition variation in a one-dimensional convection-free channel, see Schulte [11] and Hirschberg [12]. Studies on the convection effect include the research work of Faruque et al. [13], Jacqmin [14], Riley and Firoozabadi [5], and Benano-Melly et al. [15]. Shulte [11] and Hirschberg [12] have investigated the gravitational effect on the composition variation in a one-dimensional convection-free channel. Their studies show that the thermal diffusion is of the same order of magnitude as the effect of pressure diffusion. However, they neglected any convection in their analysis, which is a natural phenomenon in real cases. Faruque et al. [13] using the Firoozabadi approach compared the theoretical results with

* Corresponding author.
E-mail address: zsaghir@ryerson.ca (M.Z. Saghir).

1290-0729/$ – see front matter
doi:10.1016/j.ijthermalsci.2004.03.001

Nomenclature

c	methane mole fraction
C_p	heat capacity
D_M	molecular diffusive coefficient ..... $m^2 \cdot s^{-1}$
D_T	thermal diffusion coefficient ..... $m^2 \cdot s^{-1} \cdot K^{-1}$
D_P	pressure diffusion coefficient .... $m^2 \cdot s^{-1} \cdot Pa^{-1}$
$\vec{J}$	molar diffusive flux ..... $mole \cdot m^{-2} \cdot s^{-1}$
k	thermal conductivity ..... $W \cdot m^{-1} \cdot K^{-1}$
k_p	thermal conductivity of the solid particles ..... $W \cdot m^{-1} \cdot K^{-1}$
L_c	characteristic length
P	pressure ..... Pa
q	separation ratio
S_T	Soret coefficient, $= \frac{D_T}{D_M c(1-c)}$ ..... K^{-1}
T	temperature ..... K
t	time ..... s
u	velocity component in x-direction ..... $m \cdot s^{-1}$
v	velocity component in y-direction ..... $m \cdot s^{-1}$
$\vec{V}$	fluid velocity vector (u, v) ..... $m \cdot s^{-1}$
x	dimension in m
y	dimension in m
Le	Lewis number, $= \alpha / D_M$
Da	Darcy number, $= \kappa / L_c^2$
Ra_c	Solutal Rayleigh number, $= \frac{g\beta_c \Delta c L_c \kappa}{\nu D_M}$
Ra_T	Thermal Rayleigh number, $= \frac{g\beta_T \Delta T L_c \kappa}{\nu \alpha}$

Greek symbols

α	thermal diffusivity, $= \frac{k_e}{(\rho Cp)_f}$ ..... $m^2 \cdot s^{-1}$
β_C	solutal volume expansion coefficient
β_T	thermal volume expansion coefficient .. $1 \cdot K^{-1}$
ϕ	porosity
κ	permeability ..... m^2
μ	dynamic viscosity of the fluid mixture ..... $kg \cdot m^{-1} \cdot s^{-1}$
ν	kinematic viscosity of the fluid mixture $m^2 \cdot s^{-1}$
ρ	fluid mixture density ..... $kg \cdot m^{-3}$
ρ_m	fluid mixture molar density ..... $mole \cdot m^{-3}$
τ_f	flow characteristic time in seconds, $= \frac{L_c^{3/2}}{\sqrt{g\beta_T \Delta T \kappa}}$
τ_T	thermal characteristic time in seconds, $= \frac{L_c^2}{\alpha}$

Subscripts

o	reference quantities
c	solutal
e	effective
f	fluid mixture
m	molar quantities

the experimental data of Rutherford and Roof [10] and their results show good agreement. Three research groups have investigated the convection effect on the composition variation in hydrocarbon porous media. Jacqmin [14] simplified his modelling with the neglect of the thermal diffusion, which is an important factor we focus on, and concluded that the convection would be balanced with the composition variation based on his perturbation theory analysis. Riley and Firoozabadi [5] studied the effect of thermal, pressure, and molecular diffusions combined with natural convection in a rectangular reservoir with a prescribed linear temperature distribution. Because their research focus was on the examination of a real oil reservoir, the energy equation was omitted and a linear temperature distribution was applied in the cavity. They showed that a small amount of convection can cause the horizontal composition gradient to increase until a maximum is reached and then decay inversely proportional to the permeability of the porous medium. Benano-Melly et al. [15] examined the thermal diffusion in binary fluid mixtures subject to a lateral heating. They assumed a constant Soret coefficient in their entire numerical analysis. Their numerical results indicated a multiple convection roll flow pattern depending on the Soret coefficient value and their experimentally measured thermal diffusion coefficient was used in their numerical model. They noticed the same composition separation phenomenon as in the case of the increased permeability, or the case of convection flow, but they did not explain the mechanism behind this phenomenon.

This work investigates numerically the interaction between the thermal diffusion and the buoyancy convection in a laterally heated vertical cavity filled with a binary mixture of methane and n-butane. Our results are unique in that the Soret coefficient has not been fixed in the computational domain but rather calculated at each point of the grid as a function of the temperature, pressure and the composition of the fluid mixtures. In Section 2, the mathematical model is presented, the solution procedure is introduced in Section 3, and Section 4 presents the results. The importance of the thermal diffusion in the cavity is demonstrated to be dominant when the permeability is below a certain value and above which the buoyancy convection becomes dominant. The separation ratio is introduced to better assess the importance of each force in the cavity. Finally, Section 5 presents the conclusion drawn from this analysis.

2. Mathematical model

2.1. Mass conservation equation

In the two-dimensional domain, the mass conservation equation is written in the following form:

$$\frac{\partial \rho_m}{\partial t} + \frac{\partial (\rho_m u)}{\partial x} + \frac{\partial (\rho_m v)}{\partial y} = 0 \tag{1}$$

where ρ_m is the molar density of the mixture fluid, and u and v are the horizontal and vertical velocity components,

respectively. Because we are assuming a binary mixture, one more mass conservation equation is solved, namely:

$$\frac{\partial(\rho_m c)}{\partial t} + \frac{\partial(\rho_m u c)}{\partial x} + \frac{\partial(\rho_m v c)}{\partial y} = -\nabla \bullet \vec{J} \tag{2}$$

where $\vec{J}$ is the mass flux of the solute, methane; c is the concentration of methane. Using the transport theory, see Bird and Stewart [3], the mass flux can be expressed as follows:

$$\vec{J} = -\rho_m (D_m \nabla c + D_T \nabla T + D_p \nabla P) \tag{3}$$

where T is the temperature, P is the pressure and D_m, D_T, and D_p are the molecular diffusion, thermal diffusion and pressure diffusion coefficients, respectively. Here the thermal, molecular and pressure diffusion coefficients are functions of the temperature, pressure, and the properties of the fluid mixture. Using the irreversible thermodynamics theory, Firoozabadi and Ghorayeb [16] were able to formulate a theoretical approach to determine the dependency of those coefficients on the pressure, temperature and mixture compositions. For further details, the reader should see Faruque et al. [13] and Chacha et al. [17].

2.2. Momentum equation

In porous media, the porous matrix is assumed to be homogeneous and isotropic. Therefore the Darcy equation is applied and expressed in the following form:

$$\vec{V} = -\frac{\kappa}{\phi\mu}\left(\nabla P + \rho\vec{g}\right) \tag{4}$$

where ρ is the mass density of the fluid mixture, $\vec{g}$ is the gravitational acceleration vector, κ, μ, and ϕ are the permeability, the dynamic viscosity, and the porosity, respectively. By substituting the Darcy relation expressed in Eq. (4) into the mass conservation equation expressed in Eq. (1), the pressure differential equation becomes as follows:

$$\frac{\partial \rho_m}{\partial t} - \frac{\kappa}{\phi\mu}\frac{\partial}{\partial x}\left(\rho_m \frac{\partial P}{\partial x}\right) - \frac{\kappa}{\phi\mu}\frac{\partial}{\partial y}\rho_m\left(\frac{\partial P}{\partial y} - \rho g\right) = 0 \tag{5}$$

2.3. Energy equation

The thermal energy conservation equation is expressed as follows:

$$\frac{\partial(\rho C_p)_e T}{\partial t} + u\frac{\partial}{\partial x}\left((\rho C_p)_f T\right) + v\frac{\partial}{\partial y}\left((\rho C_p)_f T\right) = k_e\left[\frac{\partial^2 T}{\partial x^2} + \frac{\partial^2 T}{\partial y^2}\right] \tag{6}$$

where $(\rho C_p)_e$ is the effective volumetric heat capacity of the system and k_e is the effective thermal conductivity of the system. These effective physical parameters are related to the fluid properties and the solid matrix properties as follows:

$$(\rho C_p)_e = \phi(\rho C_p)_f + (1-\phi)(\rho C_p)_p \tag{7}$$

$$k_e = \phi k_f + (1-\phi)k_p \tag{8}$$

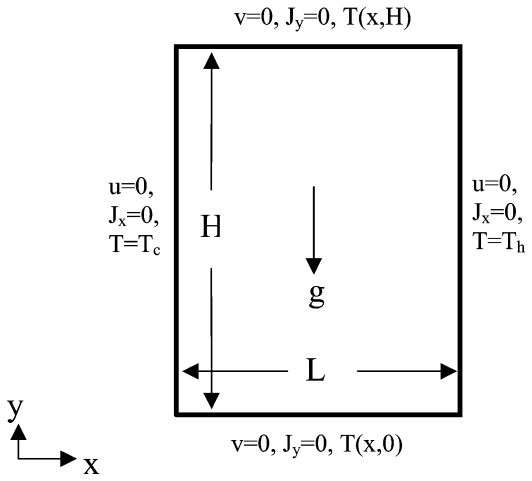

Fig. 1. Two-dimensional porous media domain and boundary conditions.

2.4. Boundary conditions

Fig. 1 depicts the problem to be solved numerically with its corresponding boundary conditions. A vertical cavity with a height H and a width L is subject to different boundary conditions on its lateral and horizontal walls. The four walls are assumed to be impermeable and non-reacting to the fluid. The two lateral walls are subject to a Dirichlet type boundary condition with a constant temperature designated by the hot temperature $T_h = 344\,^{\circ}\mathrm{C}$ and the cold temperature $T_c = 334\,^{\circ}\mathrm{C}$. On the horizontal walls a linear temperature gradient is applied. All the walls are assumed solid walls so zero velocities are maintained. The binary mixture inside the cavity consists of 20% methane (CH_4) and 80% n-butane (nC_4H_{10}). Since the Peng–Robinson Equation (EOS), see Peng and Robinson [18], is used to calculate the density variation, as well as other fluid properties, the flow is considered to be compressible. Therefore, the properties of the liquid, such as the density, viscosity and specific heat, are functions of the temperature, pressure and the fluid mixture composition. The thermal conductivity is assumed constant in the analysis. In this paper, the viscosity of the mixture is obtained with a method proposed by Herning and Zipperer [19]. It is assumed that there is no heat generation, no chemical reaction, and no interactive superficial forces acting between the porous medium particles and the liquid mixture.

3. Numerical scheme and solution procedure

Eqs. (1), (2), (5) and (6), together with their corresponding boundary conditions as depicted in Fig. 1, are solved numerically using the control volume method with a rectangular grid system. The second-order centered scheme is used in the space discretization, and a semi-implicit first-order scheme is used for the temporal integration. With respect to the non-linear convection terms, the power-law scheme, see Patankar [20], is applied in order to approach a high accuracy for the combined convection and diffusion cases.

Table 1
Parameters of the physical model

Width L of the cavity	0.5 meter
Height H of the cavity	5.0 meter
Characteristic length $L_c = \sqrt{L^2 + H^2}$	5.025 meter
Fluid mixture composition	$CH_4(20\%) + nC_4H_{10}(80\%)$
Fluid specific heat, $(C_p)_f$	2746.42 [J·kg^{-1}·K^{-1}]
Fluid thermal conductivity, k_f	0.095 [J·m^{-1}·s^{-1}·K^{-1}]
Porosity, ϕ	0.20
Permeability, κ	10^{-3}, 10, 10^4 md
Specific heat of porous medium, $(C_p)_p$	1840.0 [J·kg^{-1}·K^{-1}]
Thermal conductivity of porous medium, k_p	1.0 [J·m^{-1}·s^{-1}·K^{-1}]
Density of porous medium, ρ_p	2050.0 [kg·m^{-3}]
Reference temperature, T_0	339 K
Lateral wall temperature difference, $T_h - T_c$	10 °C
Reference pressure, P_0	11.15 MPa

The obtained linear algebraic system of equations is solved at each time step using a bi-conjugated gradient iteration method with a given convergence criterion, which has been confirmed over many tests for the required accuracy.

At the initial time step, the velocities have been set to zero in the computed domain where initial pressure and concentration are applied. The convergence criterion is set for three parameters, the pressure P, the temperature T and the concentration c, respectively. The errors between iterations are calculated as follows:

$$\gamma_\theta = \frac{1}{m \times n} \sum_{i=1}^{m} \sum_{j=1}^{n} \left| \frac{\theta_{ij}^{k,s+1} - \theta_{ij}^{k,s}}{\theta_{ij}^{k,s+1}} \right| \tag{9}$$

where θ represents the pressure, temperature and concentration, respectively, i and j represent mesh indices along the x and y directions of the domain, k denotes the time step and s is the indicator of inner iterations. The values of pressure, temperature and concentration are defined at the center of each control volume, but the velocities are defined on the surface of each control volume, or grid cell. Different mesh sizes have been tested and a 71×71 control volume has been adopted. A tight convergence criterion is applied in the time process to determine the establishment of the steady state.

The solution procedure begins by assuming the initial pressure, temperature and concentration in the mixture. The properties of the liquid, such as density (using the Peng Robinson state equation), viscosity and all three diffusion coefficients for pressure diffusion, molecular diffusion and thermal diffusion, are evaluated for each control volume based on a given temperature, pressure and composition at each time step. The calculation of the three diffusion coefficients is clearly explained in Firoozabadi et al. [6–8] and Chacha et al. [17]. Once the properties of the liquid and all three diffusion coefficients are obtained, the continuity equations (1) and (2), pressure equation (5) and the energy equation (6) can be solved with the given boundary conditions. The velocity field is updated with Eq. (4). The updated pressure, temperature, and concentration fields can be used to evaluate the liquid properties and all three diffusion coefficients again for the next time step. The convergence of the steady state is assumed when the absolute relative error of the concentration is found to be less than 10^{-8} between successive time step iterations at each control volume. The validation of this numerical scheme has been evaluated by a comparison between numerical results and experimental data given in Schulte [11]. Table 1 presents the dimensions of the cavity as well as the porosity, the permeability, the composition of the mixture and the conductivity of the mixture.

Once the velocities have been calculated, the well-known relation between the stream function and the velocities $u = \frac{\partial(\Psi)}{\partial y}$, $v = -\frac{\partial(\Psi)}{\partial x}$ is used to compute the stream function.

4. Results and discussion

Our objective, as stated earlier, is to study the importance of the convection effect, including a variable Soret coefficient as being a function of the temperature, pressure, and properties of the fluid mixture in a vertical cavity. The difference between flows with and without the Soret effect is discussed first. Then, the convection effect on the thermal diffusion process is investigated for different permeability in terms of the separation ratio and the characteristic times of the fluid flow and the thermal diffusion.

In order to investigate the significance of the Soret effect, the two-dimensional convection problem is solved with the presence of the Soret effect, as well as without the Soret effect. Jiang et al. [21] studied the convection patterns for different permeability of 10^{-3}, 10 and 10^4 md, respectively, which corresponds to a Darcy number of 3.91×10^{-20}, 3.91×10^{-16} and 3.91×10^{-13}, respectively. In the flow field, the convection due to buoyancy was shown to move fluid up along the warmer wall, push it to the top of the cavity, and finally move it down along the cold wall. The center of the flow changes accordingly as the permeability of the porous medium increases. In the presence of the Soret effect different behavior for the flow occurs. At low

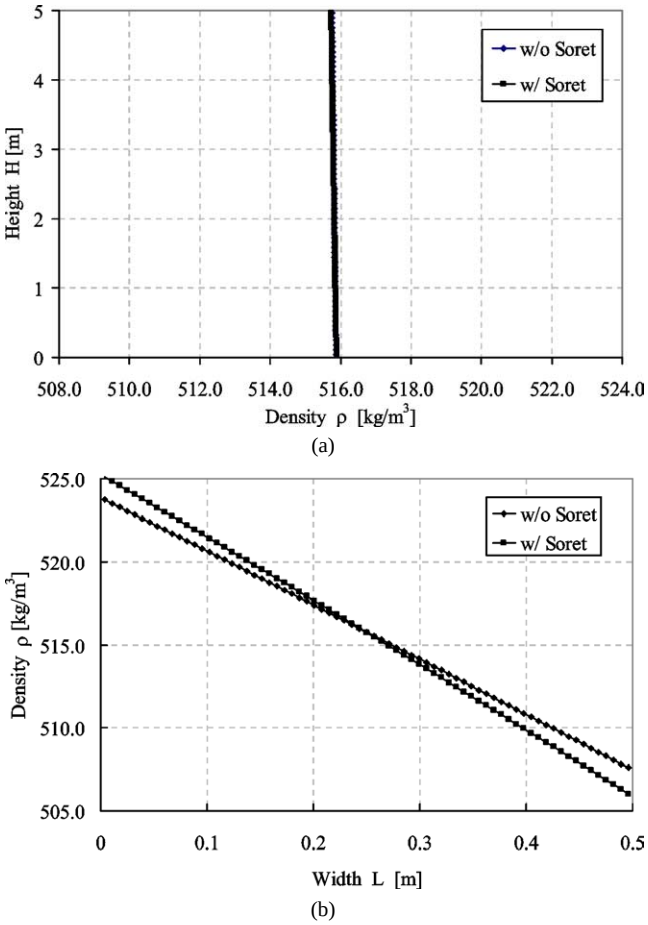

Fig. 2. Mixture density distributions at the centre of the cavity with $\kappa = 0.001$ md: (a) Vertical distribution; (b) Horizontal distribution.

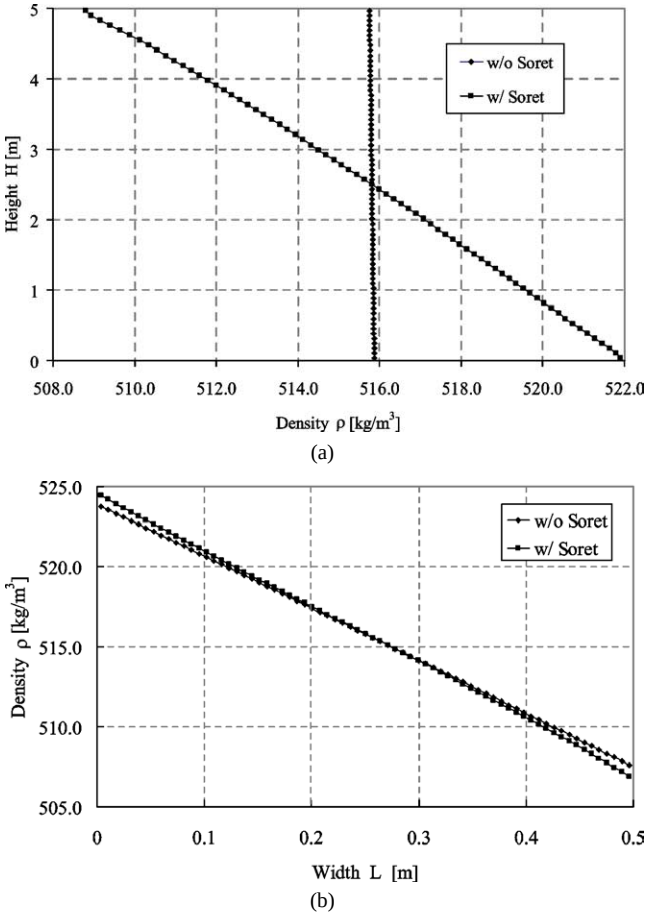

Fig. 3. Mixture density distributions along at the centre of the cavity with $\kappa = 10.0$ md; (a) Vertical distribution; (b) Horizontal distribution.

permeability, 10^{-3} md, the Soret presence is evident in the flow pattern. This significance of the Soret continues to be apparent when the value of the permeability reaches 10 md. It has been found that beyond this value of the permeability, the buoyancy convection exerts a negative effect on the composition separation and eliminates the Soret effect completely at permeability equal to 10^4 md.

4.1. Comparison of density distributions along vertical and horizontal central lines

The vertical and horizontal variation of the density at the middle of the cavity for the permeability of 10^{-3} md is presented in Fig. 2. In the vertical direction, a uniform density distribution with and without the Soret effect is observed as shown in Fig. 2(a). At such low permeabilities, the flow is weak and does not significantly affect the linear horizontal temperature distribution. The convection is so weak that there is no difference between the vertical density distributions with and without the Soret effect. Fig. 2(b) presents the density variation in the horizontal direction at the middle of the cavity. In the absence of the Soret effect a linear decrease in the density is due to the lateral heating condition. In the presence of the Soret effect, it is observed that the lighter component of the mixture, in this case the methane, migrates towards the hot side of the cavity. Therefore one expects a linear decrease of the density as shown in Fig. 2(b). The difference between these two horizontal distribution lines presents the contribution of the Soret effect, or thermal diffusion. The average density is found to be 515.8 kg·m^{-3} and the maximum deviation is 7.8 kg·m^{-3} when the Soret effect is absent and 9.2 kg·m^{-3} when both the Soret and buoyancy effects are present. Therefore, in the presence of the Soret effect there is a 15.2% increase in the density variation. The ratio between the contribution of the thermal diffusion (i.e., Soret effect) and the thermal expansion (i.e., buoyancy effect) is 0.1795, which can be considered as the ratio of two driving buoyancy forces.

The same calculation is repeated for the permeability of 10 md and as the permeability increases, convection becomes more effective in the cavity. With lateral heating conditions, the convection flow moves the lighter fluid near the hot wall to the top of the cavity and heavy fluid along the cold wall to the bottom of the cavity in the presence of the Soret effect. Fig. 3(a) shows the density variation in the vertical direction. In the absence of the Soret effect, a constant density distribution is observed. However, in the presence of

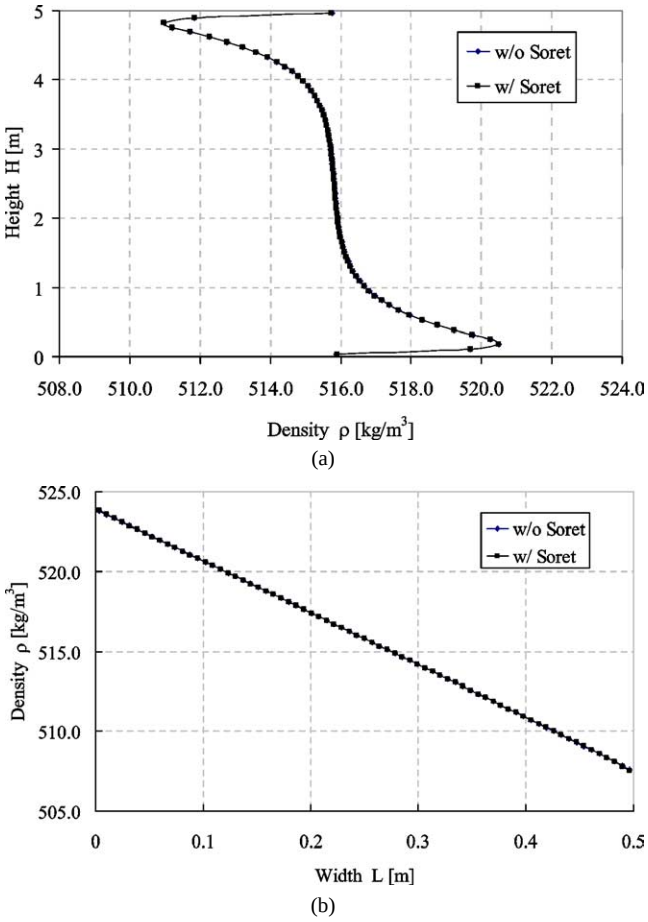

Fig. 4. Mixture density distributions at the centre of the cavity with $\kappa = 10000.0$ md: (a) Vertical distribution; (b) Horizontal distribution.

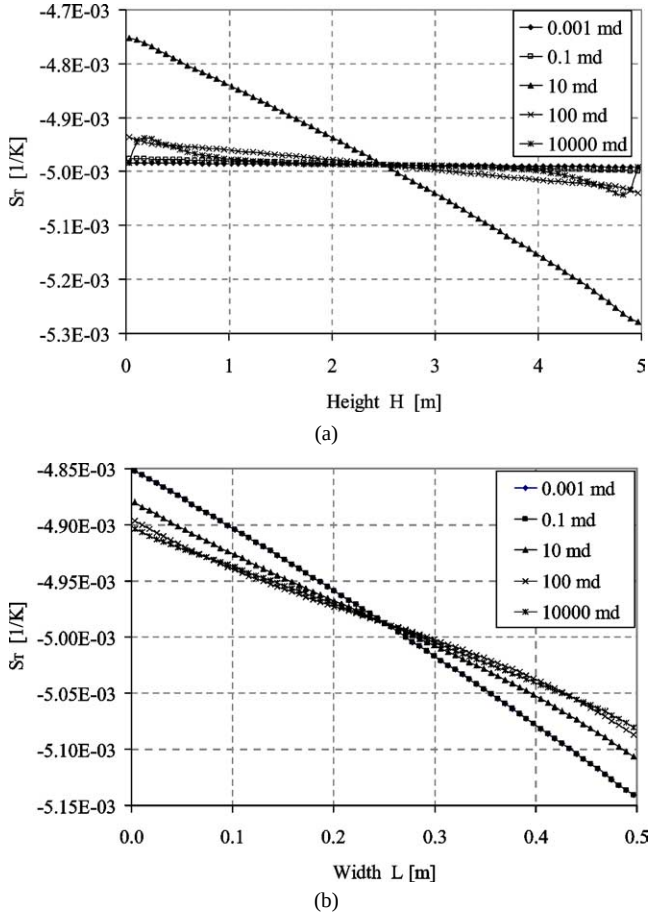

Fig. 5. Soret coefficient distribution with permeability at the centre of the cavity: (a) Vertical distribution; (b) Horizontal distribution.

the Soret effect, the vertical density distribution varies linearly. This significant change comes from the buoyancy convection. As explained earlier, the lighter component of the mixture, which is methane, migrates to the hot wall and is pushed upward by the convection to the top of the cavity. The butane being the heavy component of the mixture migrates to the cold side and is pushed downward to the bottom of the cavity. The change in the density in the vertical distribution is not observed in the case of the permeability of 10^{-3} md, due to the weak convection in the cavity. The changes in the density in the vertical direction indicate a change in the fluid composition. Fig. 3(b) presents the horizontal density variation. Without the Soret effect, the horizontal density distribution is similar to Fig. 2(a). In the presence of the Soret effect, the horizontal density distribution tends closer to the one without the Soret effect if one compares with Fig. 2(b). With an increase in the permeability, the convection becomes stronger and contributes to the vertical composition separation significantly, but decreases the horizontal composition separation slightly.

As the permeability of the porous medium increases to 10^4 md, which corresponds to a Darcy number of 3.91×10^{-13}, buoyancy convection becomes dominant and similar density variations are observed for both with and without the Soret effect, see Fig. 4. The density variation in the vertical direction is shown in Fig. 4(a). One may observe the strong convection moving counter-clockwise by examining the density variation. Moreover, Fig. 4(b) shows an identical density variation in the horizontal direction.

From the above analysis, we can conclude that the Soret effect in porous media is significantly affected by the convection flow, where the permeability, i.e., the Darcy number, is the dominant parameter.

4.2. Variation of the Soret effect and methane concentration with permeability

The Soret coefficient, which is known to be the ratio of the thermal diffusion coefficient to the molecular diffusion coefficient, is plotted as a function of the height and width at the center of the cavity for different values of permeability. This unique analysis shows the space dependence of the Soret coefficient as a function of the temperature, pressure and composition of the fluid mixture. Fig. 5(a) shows the vertical distribution of the Soret coefficient for different values of permeability. When the permeability is varied between 0.001 and 0.1 md, the Soret coefficient along the vertical direction is constant. Methane being the light

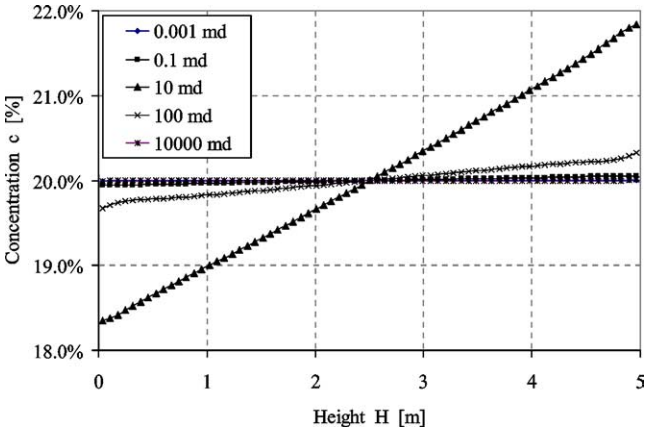

(a)

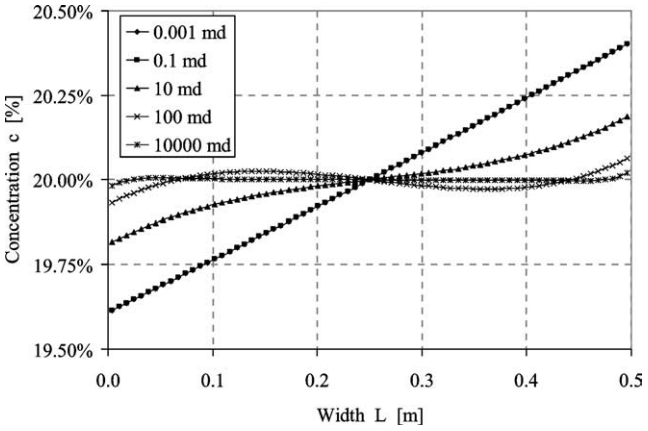

(b)

Fig. 6. Methane concentration distribution with permeability at the centre of the cavity: (a) Vertical distribution; (b) Horizontal distribution.

component does not displace in the vertical direction. When the permeability varies between 0.1 md and 100 md, a substantial variation of the vertical Soret coefficient is present, in particular at a permeability of 10 md. It is suggested that beyond 10md, the convection takes a more important role and transports methane to the top horizontal wall near the hot wall. As the permeability increases further, we note a disturbance near the horizontal wall which is due to a large temperature gradient which exists at the horizontal walls. Fig. 5(b) presents, for the same condition used above, the variation of the Soret coefficient is in the horizontal direction and it opposes the temperature distribution. It is evident that, as the permeability increases, the convection becomes effective in reducing the horizontal variation of the thermal diffusion in the cavity.

In terms of the fluid composition variation, it is found that when the permeability varies between 0.001md and 0.1md, the convection flow is weak and the Soret effect is the dominant force. Therefore, the horizontal concentration distribution is linear with a gradient proportional to the gradient of the horizontal temperature distribution. Accordingly, the vertical concentration distribution is constant as shown in Fig. 6. At this range of the permeability, the transport of the methane is shown to be effective in the horizontal direction and weak in the vertical direction. As the value of the permeability increases from 0.1 md to 100 md, the concentration of methane at the right top of the cavity increases first then decreases. The largest variation of the concentration is found at 10 md and the separation of the methane is at its maximum in the horizontal and vertical direction and we observe the maximum Soret effect with large methane migrating to the hot wall as shown in Fig. 6(a), and it is also evident in the horizontal direction, see Fig. 6(b). Beyond the point of 10 md permeability, buoyancy convection becomes dominant. When the value of permeability increases from 100 md to 10 000 md, Soret effect disappears gradually. At 10 000 md permeability, a flat methane concentration distribution in both the vertical and horizontal directions is observed. It is therefore important to examine the separation ratio term and its relationship to the permeability.

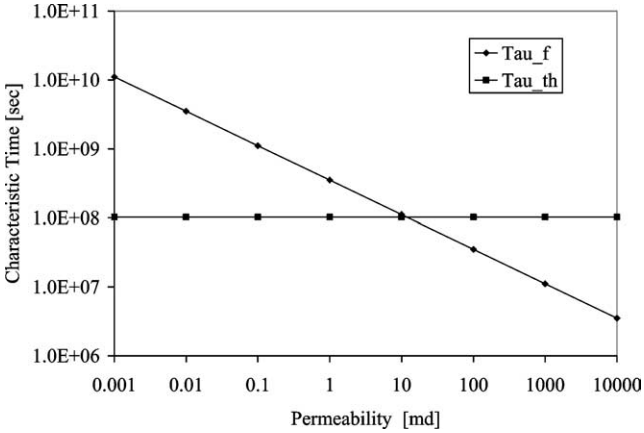

Fig. 7. The characteristic times as a function of the permeability (Tau_f $= \tau_f$, Tau_th $= \tau_{\text{th}}$).

The peak of the separation ratio at the permeability of 10 md might be explained by the fluid and thermal characteristic times as shown in Fig. 7. The characteristic time for thermal diffusion is found to be constant as the permeability increases and equal to 1.0×10^8 seconds, see Fig. 7. However, the value of the flow characteristic time, τ_f, decreases monotonically from $\tau_f = 1 \times 10^{10}$ seconds to 2.1×10^6 seconds as the permeability increases. The intersection of the fluid characteristic time and thermal characteristic time occurs at a permeability of 10 md, where the separation ratio is observed to be at its maximum value. This means that beyond this point, the fluid characteristic time is less than the thermal characteristic time and the convection becomes the dominant force in the cavity.

4.3. Separation ratio

As discussed in the previous section, the convection effect is crucial to the analysis of the thermal diffusion, or Soret effect. As the permeability of the porous medium increases, three different regimes are found based on the analysis of the density, Soret coefficient and methane concentration distributions. These three different regimes are in accordance with

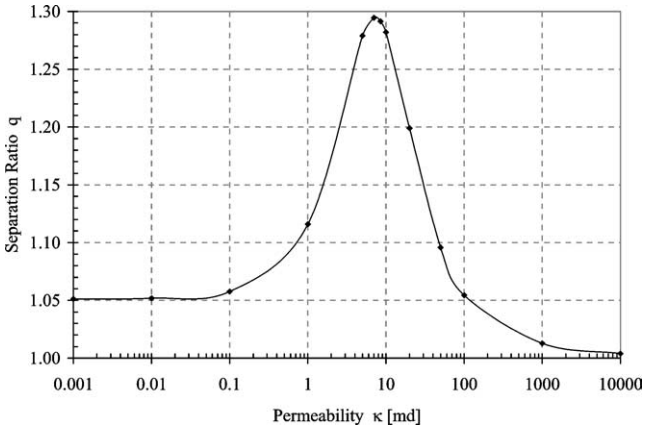

Fig. 8. The separation ratio as a function of the permeability.

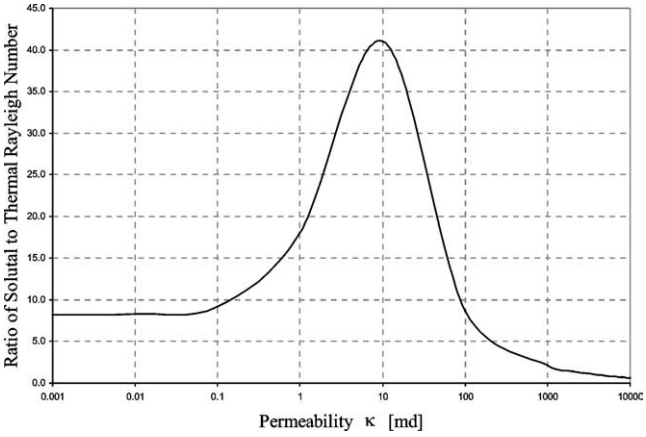

Fig. 9. Variation of the Rayleigh number as a function of the permeability.

three ranges of the permeability. To examine this phenomenon further we have chosen the separation ratio, q, as the variable, as defined below:

$$q = \frac{c_T/(1-c_T)}{c_B/(1-c_B)} \tag{10}$$

where c_T and c_B are the methane concentrations at the top and bottom horizontal walls, respectively. The variation of the separation ratio as a function of the permeability is shown in Fig. 8. For a variation of the permeability between 0.001 md and 0.1 md, the separation ratio remains constant, which is about 1.05. This separation ratio is due to the contribution of the thermal and molecular diffusion expressed in terms of the Soret effect, and the convection effect is too small to be considered. For a range of permeabilities between 1 and 100 md, we observe a peak in the separation ratio at about 10 md (i.e., Darcy number equal to 3.91×10^{-16}) with $q = 1.29$. As the permeability becomes greater than 100 md, it is observed that the separation ratio decreases rapidly. When the permeability is equal to 10^4 md, the separation ratio is close to 1, the fluid is mixed and separation does not take place. In the range of permeability greater than 10^4 md, the convection becomes dominant and the Soret effect is suppressed.

By neglecting the solutal buoyancy force and assuming constant molecular and thermal diffusion coefficients, Lorenz and Emery [22] expressed a relation between the separation ratio and the permeability as

$$\ln(q) = \frac{AL\kappa}{B\kappa^2 + C} \tag{11}$$

where A, B and C are constants in the transport equation (see Lorenz and Emery [22] for additional details). Benano-Melly et al. [15] showed that a maximum value for the separation ratio exists for a permeability $\kappa = \kappa_m$ given as follows;

$$\kappa_m = \frac{\mu D_M \sqrt{120}}{g\beta_T \Delta T L \rho} \tag{12}$$

This analytical expression predicts that the maximum separation will occur at $\kappa_m = 11.9$ md whereas our numerical calculation showed that separation occurs at $\kappa_m = 10$ md. This discrepancy between the simplified theory and the accurate numerical modeling is justified by the fact that in our case the solutal buoyancy is included and both the thermal and molecular diffusion coefficients are functions of temperature, fluid mixture and pressure. The maximum separation ratio was also analytically calculated to be equal to 1.2 compared to 1.29 which was obtained numerically. The justification for the differences between the two maximum values is similar to the permeability case as well.

Another way to study this effect is by plotting the ratio of the solutal to thermal Rayleigh numbers as a function of the permeability as shown in Fig. 9. This ratio was found to be equal to;

$$\frac{Ra_c}{Ra_T} = Le\frac{\beta_c \Delta c}{\beta_T \Delta T} \tag{13}$$

where Le is the Lewis number. In the above equation, the temperature difference is constant. The ratio of the solutal to the thermal expansion coefficients is at the limit a constant quantity. Additionally it is found that the Lewis number dependence on the temperature and the concentration is weak. However, as we demonstrated in Fig. 6(b), the concentration difference $\Delta c = c_{\max} - c_{\min}$ varies with the permeability such that it is constant for a permeability less than 0.1 md, increases between 0.1 and 10 md and then decreases with permeability greater than 10 md. Therefore the right hand term of Eq. (19) is a function of the permeability. As the permeability increases, the thermal Rayleigh number increases linearly and the solutal Rayleigh number starts with a linear variation as well and this indicates that the Soret effect is dominant. It is found that, beyond 10 md, there is a reduction in the solutal Rayleigh number and this continuous increase in the thermal Rayleigh number indicates the dominance of the buoyancy convection. The ratio of those two variations shows a profile similar to the separation ratio as depicted in Fig. 8.

5. Conclusion

Attempts have been made to investigate the convection effect on the thermal diffusion, or Soret effect, in a single-phase hydrocarbon binary mixture system. The model is based on non-equilibrium thermodynamics theory, in which all three diffusion coefficients: the molecule diffusion, the thermal diffusion and the pressure diffusion coefficients have been evaluated with time and space dependent fluid properties and compositions. In the analysis, the horizontal and vertical distributions of the mixture density, the Soret coefficient and the methane concentration in the porous medium cavity as well as separation ratio, q, have been used to analyze the behaviour of the convection effect. The results showed consistent phenomena. Especially, with the separation ratio, q, the effect of the convection flow on the thermal diffusion has been clearly presented. The main conclusion from this study is that the convection effect on the thermal diffusion in a hydrocarbon binary system could be explained in terms of the characteristic times. When the characteristic time of the convection flow, τ_f, is larger than the characteristic time of the thermal diffusion, τ_{th}, then the Soret effect is the dominant force for the composition separation in the cavity and maximum separation is reached when $\tau_f = \tau_{\text{th}}$. Finally, when $\tau_f < \tau_{\text{th}}$, the buoyancy convection becomes dominant and this corresponds to a permeability greater than 10 md. In other words, if the convection transfers information slower than the thermal diffusion, then it contributes to the Soret effect; if the convection transfers information as quickly as the thermal diffusion, then the Soret effect reaches its greatest significance; if the convection transfers information faster than the thermal diffusion, it then decreases the Soret effect until it destroys the Soret effect completely.

Acknowledgements

The authors acknowledge the full support of the Centre for Research and Space Technology (CRESTech) and the Natural Sciences and Engineering Council (NSERC).

References

[1] C. Soret, Influence de la temperature sur la distribution des sels dans leurs solutions, C. R. Acad. Sci. Paris 91 (1880) 289.

[2] K. Shukla, A. Firoozabadi, A new model of thermal diffusion coefficients in binary hydrocarbon mixtures, Ind. Eng. Chem. Res. 37 (1998) 3331.

[3] R.B. Bird, W.E. Stewart, Transport Phenomena, Wiley, New York, 2002.

[4] E.L. Dougherty, H.G. Drickamer, Thermal diffusion and molecular motion in liquids, J. Phys. Chem. 59 (1955) 443.

[5] M.F. Riley, A. Firoozabadi, Compositional variation in hydrocarbon reservoirs with natural convection and diffusion, AIChE J. 44 (1998) 452.

[6] K. Ghorayeb, A. Firoozabadi, Modeling of multicomponent diffusion and convection in porous media, SPE J. 5 (2000) 158.

[7] K. Ghorayeb, A. Firoozabadi, Features of convection and diffusion in porous media for binary systems, J. Canad. Petroleum Technol. 40 (2001) 21.

[8] K. Ghorayeb, A. Firoozabadi, Molecular, pressure and thermal diffusion in nonideal multicomponent mixtures, AIChE J. 46 (2000) 883.

[9] S.R. De Groot, Non-Equilibrium Thermodynamics, North-Holland, Amsterdam, 1984.

[10] W.M. Rutherford, J.G. Roof, Thermal diffusion in methane n-butane mixture in the critical region, J. Phys. Chem. 63 (1959) 1506.

[11] A.M. Schulte, Compositional variation whiten a hydrocarbon column due to gravity, SPE 9235 presented at the SPE Annual Technical conference and Exhibition, Dallas, TX, September 21–24, 1980.

[12] A. Hirschberg, Role of asphaltenes in compositional grading of a reservoir's fluid column, J. Petroleum Technol. AIME 285 (1988) 89.

[13] D. Faruque, M. Chacha, M.Z. Saghir, K. Ghorayeb, Compositional variation considering diffusion and convection for binary mixture in porous media, J. Porous Media 7 (2) (2004) 1–19.

[14] D.J. Jacqmin, Interaction of natural convection and gravity segregation in oil/gas reservoirs, SPE Res. Engrg. Trans. AIME 289 (1990) 233.

[15] L.B. Benano-Melly, J.P. Caltagirone, B. Faissat, F. Montel, P. Costeseque, Modelling Soret coefficient measurement experiments in porous media considering thermal and solutal convection, Internat. J. Heat Mass Transfer 44 (2001) 1285.

[16] A. Firoozabadi, K. Ghorayeb, K. Shukla, Theoretical model of thermal diffusion factors in multicomponent mixtures, AIChE J. 46 (2000) 892.

[17] M. Chacha, D. Faruque, M.Z. Saghir, J.C. Legros, Thermodiffusion in binary mixture in the presence of g-jitter, Internat. J. Thermal Sci. 41 (2002) 899.

[18] D.Y. Peng, D.B. Robinson, A new two-constant equation of state, Ind. Engrg. Chem. Fund. 15 (1976) 59.

[19] F. Herning, L. Zipperer, Calculation of the viscosity of technical gas mixtures from the viscosity of individual gases, Gas u. Wasserfach 79 (1936) 69.

[20] S.V. Patankar, Numerical Heat Transfer and Fluid Flow, Taylor and Francis, 1980.

[21] C.G. Jiang, M.Z. Saghir, M. Kawaji, K. Ghorayeb, Permeability effect in a vertical porous cavity with Soret contribution, in: NATO Conference on Emerging Technology, Romania, June 9–20, 2003.

[22] M. Lorenz, A.H. Emery, The packed thermal diffusion column, Chem. Engrg. Sci. 11 (1959) 16.